Preliminary Data-Subject to Revision

A Theoretically-Based Calibration and Evaluation Procedure for Vibrating-Tube Densimeters[1,2]

C. D. Holcomb[3] and S. L. Outcalt[3]

[1] Paper presented at the Thirteenth Symposium on Thermophysical Properties, June 22-27, 1997, Boulder, Colorado, U.S.A.

[3] National Institute of Standards and Technology, Physical and Chemical Properties Division, 325 Broadway, Boulder, CO 80303

ABSTRACT

A calibration procedure for vibrating-tube densimeters is developed which properly accounts for the effects of pressure and temperature on the Young's modulus and internal volume of the vibrating-tube. The calibration equation is based on the theoretical dependence of the Young's modulus, the compressibility, and the thermal expansion coefficient of the tube material on temperature and pressure. Experience shows that the vibration period of the evacuated tube can shift a small amount over time as the stresses in the tube and welds age. Therefore, the calibration equation is formulated relative to a vacuum reference period to adjust for these shifts.

The vibrating-tube densimeter is a very precise instrument, and can be a very accurate instrument when calibrated correctly. However, improper calibration of a vibrating-tube densimeter can result in systematic deviations under certain conditions, and larger than expected experimental uncertainties. Calibrating over larger-than-necessary temperature, pressure, or density ranges can increase the experimental uncertainty of the measurement. Using additional terms in the calibration equation or using an equation that does not include correct temperature and pressure dependence can introduce overfitting errors and systematic errors and reduce the accuracy of the measurements.

A first-order approximation of our theoretically-based equation is also derived. The calibration procedure is accomplished in two parts. First, the evacuated tube is calibrated to characterize the elastic modulus and linear thermal expansion coefficient of the tube as a function of temperature. Second, the change of the internal volume of the tube with temperature and pressure is characterized using two or more well-characterized calibration fluids. A procedure for choosing calibration fluids, temperatures, and pressures for the calibration points is developed. The densimeters are thoroughly tested with a variety of gases and liquids to show the validity of the equation over the calibration range .

KEYWORDS: Vibrating-tube Densimeter, Calibration Equation

1. INTRODUCTION TO VIBRATING-TUBE DENSIMETERS

Thermophysical property data are paramount for the efficient design of chemical processes. Calculations for chemical process flow conditions, material throughput, and hydrostatic stresses require gas and liquid density

data. However, accurate density data are available for only a relatively few industrially important fluids and fluid mixtures. Although many methods of measuring fluid density exist, the methods with the highest degree of accuracy are time consuming. The faster methods of measuring fluid density are less accurate. The vibrating-tube method of measuring fluid density is one method that can be fast and accurate depending on calibrations with fluids of known density.

Properly designed vibrating-tube densimeters can be stable, repeatable, and precise [1,2], although the measurement is relative not absolute. Relative measurements do not directly measure the desired property, but instead rely on the measurement of a property related to the desired property. For the vibrating-tube densimeter, the resonant frequency of the tube filled with the fluid is the measured property. The density is calculated from the resonant frequency, temperature, and pressure using a calibration equation. In this paper, we develop a calibration equation for the vibrating-tube densimeter based on sound theories and assumptions and tested for consistency. We incorporate the theory of vibration and the theory of deformation of a material. We derive an operating equation that is valid at any temperature and pressure below the elastic threshold of the densimeter. We use our understanding of the operating equation to determine the coefficients in the equation. Before the model is developed, a review of the design and operation of a vibrating-tube densimeter is given.

2. BASIC THEORY OF A VIBRATING-TUBE DENSIMETER

Many vibrating-tube densimeters consist of a hollow tube bent in a U or a V shape, two coils of wire, two magnets, a base, a frequency counter, and a current source. Figure 1 shows a schematic diagram of a vibrating-tube densimeter. The isolating block of the densimeter clamps the ends of the tube and isolates the tube from external vibrations. At the free section of the tube, two small magnets are mounted. On the base of the densimeter two coils extend upward around the magnets. A current source is connected to the drive coil. A frequency counter is connected to the pick-up coil.

One method of operating the densimeter is to activate the drive coil with a pulse from the current source. The drive coil exerts a force on the magnet inside it, causing it to act like a hammer hitting the tube. A feedback loop optimizes the time between drive pulses. The tube vibrates transversely, and the second magnet moves in and out of the pick-up coil. The movement of the second magnet induces a current at a frequency equal to that of

the vibrating tube. The frequency counter analyzes the signal from the pick-up coil and measures the resonant frequency of the tube. As the density of the fluid in the tube changes, the resonant frequency of the tube changes.

Most vibrating-tube densimeters are constructed from small thin-walled tubes. Therefore, only fluids of relatively low viscosities can be measured accurately in vibrating-tube densimeters. Because of this limitation, the viscous damping effect of the fluid on the vibration is assumed to be negligible [3]. This assumption is useful because it significantly simplifies the operating equation.

3. TEMPERATURE AND PRESSURE EFFECTS ON A HOLLOW TUBE.

Unlike damping, the effects of temperature and pressure on the system are not negligible. The temperature and pressure of the vibrating tube affect the resonant frequency in three ways: (1) the tube expands with increasing temperature, lowering the resonant frequency, (2) the tube becomes less stiff with increasing temperature, lowering the resonant frequency, and (3) the tube radius expands and the tube length decreases with increasing pressure, changing the resonant frequency.

First, we examine changes in the tube's dimensions as a function of temperature. The linear thermal expansion coefficient, "(T), of the tube material relates the effects of temperature on the dimensions of the tube. For solids, "(T) is defined as $(1/l_o)(dl/dT)$, where l_o is the reference linear dimension[4]. Most handbooks assume "(T) can be treated as pressure independent and report a $"_{avg}(T)$ which is equal to $(\int_{T_o}^{T} \alpha(T)dT)/(T - T_o)$. When "(T) is a constant then "(T) = $"_{avg}(T)$. The linear expansion coefficient reported in handbooks are for unstressed materials. Because the tube is extruded, bent, and welded, the coefficients reported in the handbook are only approximate for the densimeter. To calculate the change in length [L(T,P)] or inner radius [R_i(T,P)] of the hollow tube as functions of temperature (T) at a fixed pressure (P), we integrate the linear expansion coefficient from the reference temperature (T_o) to the final temperature:

$$R_i(T,P) = R_i(T_o,P)\left(1 + \int_{T_o}^{T} \alpha(T)\, dT\right) = R_i(T_o,P)\left(1+\alpha_{avg}(T)(T-T_o)\right), \tag{1}$$

$$L(T,P) = L(T_o,P)\left(1 + \int_{T_o}^{T} \alpha(T)\, dT\right) = L(T_o,P)(1+\alpha_{avg}(T)\ (T-T_o)). \tag{2}$$

The elasticity of the tube is a function of temperature and is related to the Young's modulus, E(T). E(T) is related to the stiffness of the tube and the elastic deformation of the tube with pressure. The actual functional forms used for $\alpha_{avg}(T)$ and E(T) depend on the temperature range of the calibration.

The pressure effects on the internal volume of the tube are more complicated than the temperature effects. The common approximations for the change of the internal radius and the length of a tube are found in the Mechanical Engineering Handbook [5]. The pressure affects the radius and the length in different ways. The inner radius of the tube increases with increasing pressure, while the length of the tube decreases. The changes in the length and radius are related to the membrane stresses of a thin-walled tube under pressure, which are used to calculate the change in the radius and length [5]. Equations (3) and (4) below are approximations that relate the changes of the radius and length with pressure, the wall thickness of the tube [$t_w(T,P)$], and the Poisson ratio (ν). These are approximate equations which assume that the deformation is elastic and that E(T) is independent of pressure.

$$R_i(T_o,P) = R_i(T_o,0)\left(1+\frac{P\left(\frac{1}{2}+\frac{R_i(T_o,0)}{t_w(T_o,0)}\right)}{E(T_o)}\left(1-\frac{\nu}{2}\right)\right), \tag{3}$$

$$L(T_o,P) = L(T_o,0)\left(1-\frac{\nu P\left(\frac{1}{2}+\frac{R_i(T_o,0)}{t_w(T_o,0)}\right)}{2E(T_o)}\right). \tag{4}$$

We reference the changes in the tube's dimensions as a function of temperature and pressure to the dimensions at a reference temperature and vacuum. We calculate the change in the tube's dimensions by traveling along a path of constant pressure (P=0) and then along a path of constant temperature. Because the inner radius and the wall thickness both change by a factor of $(1+\alpha_{avg}(T)(T-T_o))$ the ratio does not change. By combining equations (1) and (3) and equations (2) and (4), we have

$$R_i(T,P) = R_i(T_o,0)\left(1+\frac{P\left(\frac{1}{2}+\frac{R_i(T_o,0)}{t_w(T_o,0)}\right)}{E(T)}\left(1-\frac{\nu}{2}\right)\right)\left(1+\alpha_{avg}(T)\,(T-T_o)\right) \wedge \tag{5}$$

$$L(T,P) = L(T_o,0)\left(1-\frac{\nu P\left(\frac{1}{2}+\frac{R_i(T_o,0)}{t_w(T_o,0)}\right)}{2E(T)}\right)\left(1+\alpha_{avg}(T)(T-T_o)\right). \tag{6}$$

4. TRANSVERSE VIBRATING-ROD MODEL

The vibrating rod is physically similar to the vibrating tube because both ends are clamped, the mass is evenly distributed along the length of the rod, and the rod is vibrating in a transverse mode. For the vibrating-rod model, we make the following assumptions: (1) the resonant frequency is the only important frequency, (2) the forcing function is zero after the initial pulse to the drive coil, and (3) the damping effects are negligible. With these assumptions, Newton's equation of motion for a vibrating rod with density, $D_R(T,P)$, cross-sectional area, A(T,P), second moment of inertia, I(T,P), vertical displacement, Y(Z,t) at position, Z, and time, t, is [6] is:

$$E(T)I(T,P)\frac{\partial^4 Y(Z,t)}{\partial Z^4} + \rho_R(T,P)A(T,P)\frac{\partial^2 Y(Z,t)}{\partial t^2} = 0. \tag{7}$$

The boundary conditions necessary for having the rod clamped at both ends are Y(0,t) = 0, Y(L(T,P),t) = 0, MY/MZ (0,t) = 0, and MY/MZ (L(T,P),t) = 0 [6,7]. We apply a separation-of- variables technique to equation (7) to solve for Y(Z,t) in terms of unknown coefficients (C_i) and the generalized frequency of the rod (O):

(8)

From the boundary conditions we find [6,7]:

$$\cos(\beta(T,P)L(T,P))\ \cosh(\beta(T,P)L(T,P)) = 1. \tag{9}$$

We let $$_1 which is a unique constant be the first nonzero solution of equation (9):

$$\beta_1 = \left(\omega_n(T,P)\left(\frac{\rho_R(T,P)A(T,P)}{E(T)I(T,P)}\right)^{1/2}\right)^{1/2} L(T,P)\ , \tag{10}$$

where $O_n(T,P)$ = resonant frequency

We solve equation (10) for $D_R(T,P)$. The overall density of the tube is equal to the sum of the mass of the tube (m_T) divided by the total volume [V(T,P)] plus the density of the fluid [$D_F(T,P)$] times the internal volume of the tube [$V_i(T,P)$] divided by the total volume. Using V(T,P) = A(T,P)L(T,P), we obtain

$$\rho_F(T,P) = \frac{\beta_1^4 E(T) I(T,P)}{L^3(T,P)\omega_n^2(T,P) V_i(T,P)} - \frac{m_T}{V_i(T,P)} \tag{11}$$

Equation (11) is the basic operating equation. We incorporate a reference point to simplify the calibration procedure and to reduce the effect of the assumptions used in the model. We evaluate equation (1) at vacuum [$D_F(T,P)=0$] and at the reference temperature T_o and solve for $o_n2(T_o,0)$, to obtain

$$\omega_n^2(T_o,0) = \frac{\beta_1^4 E(T_o) I(T_o,0)}{L^3(T_o,0) m_T}. \tag{12}$$

The quantity, $o_n2(T_o,0)$, is measured periodically to check the densimeter's stability.

Combing equation (11) and (12), we obtain

$$\rho_F(T,P) = \frac{m_T}{V_i(T,P)}\left(\frac{L^3(T_o,0)E(T)I(T,P)\omega_n^2(T_o,0)}{L^3(T,P)E(T_o)I(T_o,0)\omega_n^2(T,P)} - 1\right). \tag{13}$$

Considering I(T,P) is proportional to $R_i^4(T,P)$ [8], the circular cross-section of the tube and combining equations (5), (6), and (13), we obtain:

$$\rho_F(T,P) = \left(\frac{\omega_n^2(T_o,0)\left(1+\frac{P\left(\frac{1}{2}+\frac{R_i(T_o,0)}{t_w(T_o,0)}\right)}{E(T)}\left(1-\frac{\nu}{2}\right)\right)^4 \left(1+\alpha_{avg}(T)(T-T_o)\right)E(T)}{\omega_n^2(T,P)\left(1-\frac{\nu P\left(\frac{1}{2}+\frac{R_i(T_o,0)}{t_w(T_o,0)}\right)}{2E(T)}\right)^3 E(T_o)} - 1\right) \left(\frac{m_T}{R_i^2(T_o,0)\left(1+\frac{P\left(\frac{1}{2}+\frac{R_i(T_o,0)}{t_w(T_o,0)}\right)}{E(T)}\left(1-\frac{\nu}{2}\right)\right)^2 \left(1+\alpha_{avg}(T)(T-T_o)\right)^3 L(T_o,0)\left(1-\frac{\nu P\left(\frac{1}{2}+\frac{R_i(T_o,0)}{t_w(T_o,0)}\right)}{2E(T)}\right)\pi}\right). \tag{14}$$

The functional forms that represent $\alpha_{avg}(T)$ and E(T) as functions of temperature with coefficients A_i and E_i for solids from approximately 150 K until the melting point or a phase transition are below [9,10]:

$$\alpha_{avg}(T) = A_1 + A_2 T + A_3 T^2, \wedge \tag{15}$$

$$E(T) = E_1 - \frac{E_2}{\exp(-E_3/T) - 1}. \tag{16}$$

Equations (14-16) contain the information necessary to calibrate a densimeter over a very wide range of temperature and pressure. There are nine unknowns and one measured parameter in equation (14). The measured parameter is $\omega_n(T_o,0)$. There are six coefficients for E(T) and $\nu_{avg}(T)$. In addition to the Poisson ratio, κ, there are two unknown groups of parameters. The two groups include the tube's dimensions and mass, $(m_T/R_i^2(T_o,0)\,L(T_o,0)\beta)$ and $(0.5+R_i(T_o,0)/t_w(T_o,0))$.

5. FIRST-ORDER APPROXIMATION

For most applications where the temperature, pressure, and density ranges are moderate, the complexity of equations (16-18) is unnecessary. Over a temperature range of 273-423 K and pressures to 14 MPa, a first-order approximation for the pressure and temperature corrections for the tube dimensions and a second-order approximation in temperature corrections for the resonant frequency at vacuum of these equations is sufficient. The first step in the approximation is to assume that $\nu_{avg}(T)$ is a constant and E(T) is linear in temperature.

The coefficients for E(T) and $\nu_{avg}(T)$ can be determined from resonant frequencies measured at vacuum at different temperatures. Using fluid density data would introduce additional error into the coefficients for E(T) and $\nu_{avg}(T)$, since they are properties of the tube material. As a check, the coefficients determined for E(T) and $\nu_{avg}(T)$ should be used to calculate E(T) and $\nu_{avg}(T)$ at a specific temperature and compared to literature results for the tube material. We evaluate equation (14) at vacuum, where $D_F(\rho,0)$ is zero, solve for the normalized frequencies, substitute our approximations for E(T) and $\nu(T)$, and obtain the following expression

$$\frac{\omega_n^2(T,0)}{\omega_n^2(T_o,0)} = \left(\frac{\left(1+\alpha_{avg}(T)\ (T-T_o)\right)E(T)}{E(T_o)} \right) = \left(\frac{(1+A_1(T-T_o))(E_1+E_2T)}{(E_1+E_2T_o)} \right)$$
$$= [1+A_1(T-T_o)][1+E_3(T-T_o)], \tag{17}$$

where $E_3 = E_2/(E_1 + E_2T_o)$.

We define coefficients for the three remaining unknown groups of parameters. B_1 is equal to $(m_T/R_i^2(T_o,0)L(T_o,0)\beta)$, B_2 is equal to $(0.5+R_i(T_o,0)/t_w(T_o,0))$; and B_3 is equal to κ. We substitute equation (17) and these coefficients into equation (14), and simplify.

$$\rho_F(T,P)=\left(\frac{\omega_n^2(T_o,0)\left(1+\frac{PB_2\left(1-\frac{B_3}{2}\right)}{(E_1+E_2T)}\right)^4\left(1+A_1(T-T_o)\right)\left(1+E_3(T-T_o)\right)}{\omega_n^2(T,P)\left(1-\frac{PB_2B_3}{2(E_1+E_2T)}\right)^3}-1\right)\left(\frac{B_1}{\left(1+\frac{PB_2\left(1-\frac{B_3}{2}\right)}{(E_1+E_2T)}\right)^2\left(1+A_1(T-T_o)\right)^3\left(1-\frac{PB_2B_3}{2(E_1+E_2T)}\right)}\right). \tag{18}$$

All of the corrections to the radius and length of the tube are small. We expand the equation, divide through by the denominators, and keep only the first order pressure and temperature corrections for the tube dimensions and the second order temperature corrections for the resonant frequency at vacuum. This produces the following equation

$$\rho(T,P)=\left(\frac{\omega_n^2(T_o,0)\left(1+PB_2E_1\left(4-0.5B_3\right)\right)\left(1+A_1(T-T_o)\right)\left(1+E_3(T-T_o)\right)}{\omega_n^2(T,P)}-1\right)B_1\left(1+PB_2E_1\left(1.5B_3-2\right)\right)\left(1-\ 3A_1(T-T_o)\right). \tag{19}$$

We expand the equation further and eliminate any PT corrections to the tube dimension term which are effectively second-order corrections:

$$\rho(T,P)=\left(\frac{\omega_n^2(T_o,0)\left(1+A_1(T-T_o)\right)\left(1+E_3(T-T_o)\right)B_1}{\omega_n^2(T,P)}\right)-B_1-B_1PB_2E_1\left(1.5B_3-2\right)+B_13A_1(T-T_o). \tag{20}$$

Equation (20) is of the same form as a calibration equation used by Niesen [11]. The difference is that Niesen's equation has one more coefficient:

$$\rho(T,P)=\left(\frac{\omega_n^2(T_o,0)(A'_1+A'_2T+A'_3T^2)}{\omega_n^2(T,P)}\right)+A'_4+A'_5P+A'_6T. \tag{21}$$

If the B_1 coefficient in the first term of equation (20) is set equal to a new coefficient B_4, then equations (20) and (21) are equivalent. Niesen [12] obtained equation (21) by eliminating unnecessary terms with a maximum

likelihood algorithm in a series expansion presented in reference [13]. The series expansion in reference [13] apparently lacks any theoretical basis. The equation is presented below[12]:

$$\rho_F = \sum_{ijk} a_{ijk} \omega_n^{-i}(T,P) T^j P^k \tag{22}$$

The power of the frequency is allowed to vary over the summation. In our equation, the only terms for the frequency are zero and inverse second order terms. These terms come directly from the solution of the vibrating rod equation. Our calibration procedure requires vacuum data and specifies which coefficients depend on the tube properties. The calibration procedure recommended for use with equation (22) does not require vacuum data and does not specify which terms are dependent on the tube properties [13]. Niesen allowed her calibration data to eliminate unnecessary or physically incorrect terms which allowed the physical behavior of the tube produce her calibration equation[12]. Using equation (22) without vacuum data and with too many terms can result in overfitting, systematic deviations under certain conditions, and larger than expected experimental uncertainties. These potential problems will be shown is a future paper.

6. CALIBRATION PROCEDURES

The two coefficients for E(T) and $\eta_{avg}(T)$ are determined from frequencies measured at vacuum at temperatures from 273 to 423 K. The four remaining coefficients must be determined from data at various densities, pressures, and temperatures. Some of the optimal calibration fluids for temperatures from 273 to 423 K and pressures to 14 MPa for which we have accurate single-phase pressure-density-temperature data include nitrogen, propane, butane, water, toluene, and HFC-152a. The relationship between the frequencies and the density at a given temperature and pressure is linear. Therefore, two calibration fluids, one at the lower limit of the density range and one at the upper limit, are required to define the relationship. This assumption is valid only when the temperature and pressure effects on the tube are accurately determined. Therefore, the calibration data must include a range of pressures and temperatures within the desired calibration range for both of the calibration fluids.

We use our densimeters to measure vapors and liquids with densities from 0.1 to 1200 kg/m^3. We have previously used nitrogen and water for calibration fluids because of the large quantities of accurate density data

that are available for these fluids. We will use toluene or HFC-152a in place of water in the future because these fluids are easier to remove from the densimeters after the calibration, and new relatively high accuracy density data are available for the calibration.

Figure 2 shows the comparisons of measured densities for ethane, propane, n-butane, and HFC-152a using equation (20) as the calibration equation and nitrogen and water as the calibration fluids. The temperatures for the calibration data were at 20 K intervals from 273 to 423 K and the pressures were at 3.4 MPa intervals. The density data for the test fluids covered a temperature range from 295 to 409 K and pressures up to 3.5 MPa. All of the data were obtained on the same two densimeters. The experimental uncertainty for the measurements is ±0.5 kg/m^3 based on the root mean square deviation of the fit to the calibration data. The average uncertainty for the liquid and vapor density correlations are ±0.3 kg/m^3 and ±1.0 kg/m^3, respectively [18-21]. The data agree with the correlations within the combined uncertainties. Although equation (14) is more difficult to implement because of its complexity, it could be used as the calibration equation and would probably decrease the experimental uncertainty, assuming that the densimeter is properly constructed so the resonant frequency at the reference point is stable and repeatable.

7. SUMMARY

This development of a calibration equation and procedure offers several advantages over other efforts. We show that by properly incorporating the temperature and pressure effects and by incorporating a reference point, many of the model-dependent inaccuracies are reduced. We indicate when approximations are appropriate for the temperature dependence of the Young's modulus and the linear thermal expansion coefficient. We specify how to determine the coefficients to avoid introducing unnecessary inaccuracies. The operating equation and calibration procedure allow us to attain low experimental uncertainties with the vibrating-tube densimeter.

8. FUTURE WORK

A subsequent paper will demonstrate the validity of equation (14) as the calibration equation with higher order terms for $\varepsilon_{avg}(T)$ and E(T). The paper will also demonstrate the potential problems of using more than 6 coefficients in a series expansion and of excluding vacuum data from the calibration data. We will also

discuss design considerations for the densimeters and experimental uncertainties that depend on the densimeter design and the signal analysis.

REFERENCES

1. H. J. Albert and R. H.Wood, *Rev.Sci. Instrum*. **55 (4)**: 1984, 589 (1984).
2. P. Picker, E. Tremblay, and C. Jolicoeur, *J. of Sol.Chem.*, **3(5):** 377 (1974).
3. J. R. Noles, ?Vapor-liquid equilibria of solvating binary mixtures," PhD. Thesis, Cornell University, pp. 46-61. (1991).
4. ASTM, ?1994 Annual Book of ASTM Standards:General Test Methods, Nonmetal; Laboratory Apparatus; Statistical Methods; Forensic Sciences" ASTM Volume 14.02, p.133. (1994).
5. L. S. Mark, Mechanical Engineer's Handbook, McGraw-Hill, p.421 (1951).
6. C. R. Wylie and L. C.Barrett, Advanced Engineering Mathematics. McGraw-Hill Book Company, 5th ed., pp. 469, 516-518 (1982).
7. R. Courant and D. Hilbert, Methods of Mathematical Physics, Wiley-Interscience Publication, Volume 1, pp. 295-297 (1937).
8. T. Retsina, S. M. Richardson, and W. A. Wakeham, *Applied Scientific Research*, **43**: 127 (1986)
9. R. H. Perry, D. W. Green, and J. O. Maloney, Perry's Chemical Engineers' Handbook, 6th ed., McGraw-Hill Book Co., p.3-104 (1984).
10. M. Lei, and H. Ledbetter, ?Oxides and Oxide Superconductors: Elastic and Related Properties" Natl. Inst. Stand. Technol. Interagency Report 3980, p.28.
11. V. Niesen, *J. Chem. Thermo.* **21:** 915 (1989)
12. V. Niesen, (private communication).
13. Anton Paar, User Manual for ?DMA 512 P Density Measuring Cell for High Pressures and High Temperatures." Anton Paar,p. 21 (1995).
14. C. D. Holcomb, unpublished data, 1993.
15. C. D. Holcomb, J.W. Magee, and W.M.Haynes, ?Density Measurements on Natural Gas Liquids," Gas Processors Association Research Report, RR-147 (1995).
16. V. Niesen and J. C. Rainwater, *J. Chem. Thermo.* **22:** 777 (1990).
17. C. D. Holcomb, V. G. Niesen, L.J. Van Poolen, and S.L. Outcalt, *Fluid Phase Eq.* **91:** 145 (1993).

18. R. D. Goodwin, H. M. Roder, and G. C. Straty, ‹Thermophysical Properties of Ethane from 90 to 600 K at Pressures to 700 Bar," Natl. Bur. Stands. (U.S.) Tech. Note 684 (1976).

19. R. D. Goodwin and W. M. Haynes, ?Thermophysical Properties of Propane from 85 to 700 K at Pressures to 70 kPa" Natl. Bur. Stands. (U.S.) Monograph 170 (1982).

20. W. M. Haynes and R. D. Goodwin, ?Thermophysical Properties of Normal Butane from 135 to 700 K at Pressures to 70kPa," Natl. Bur. Stands. (U.S.) Monograph 169 (1982).

21 M. O. McLinden and S. A. Klein, Proc. 6th Int. Refrig. Conf. at Purdue, West Lafayette, IN, July 23-26, 409 (1996).

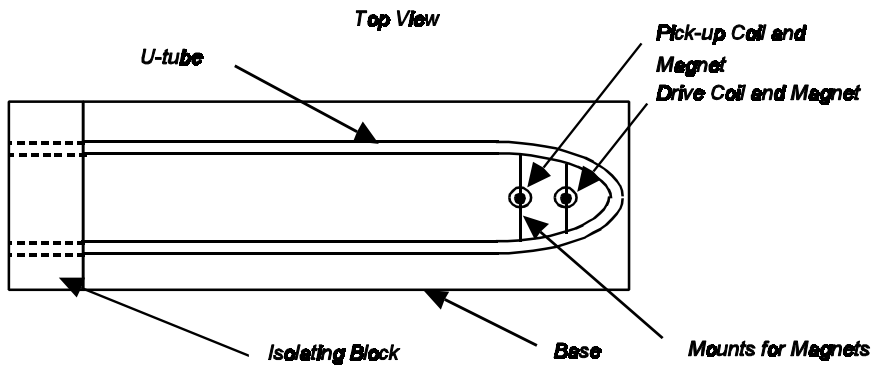
Top View
U-tube
Pick-up Coil and Magnet
Drive Coil and Magnet
Isolating Block
Base
Mounts for Magnets

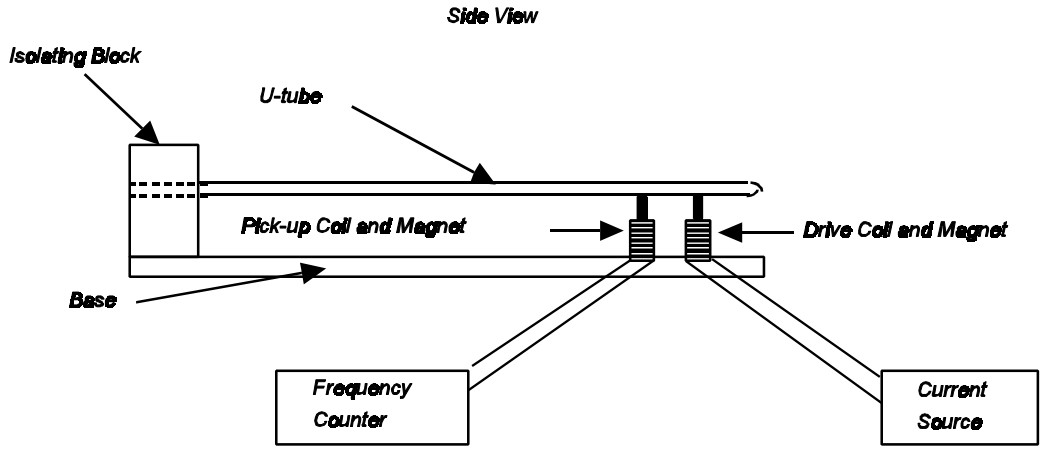
Side View
Isolating Block
U-tube
Pick-up Coil and Magnet
Drive Coil and Magnet
Base
Frequency Counter
Current Source

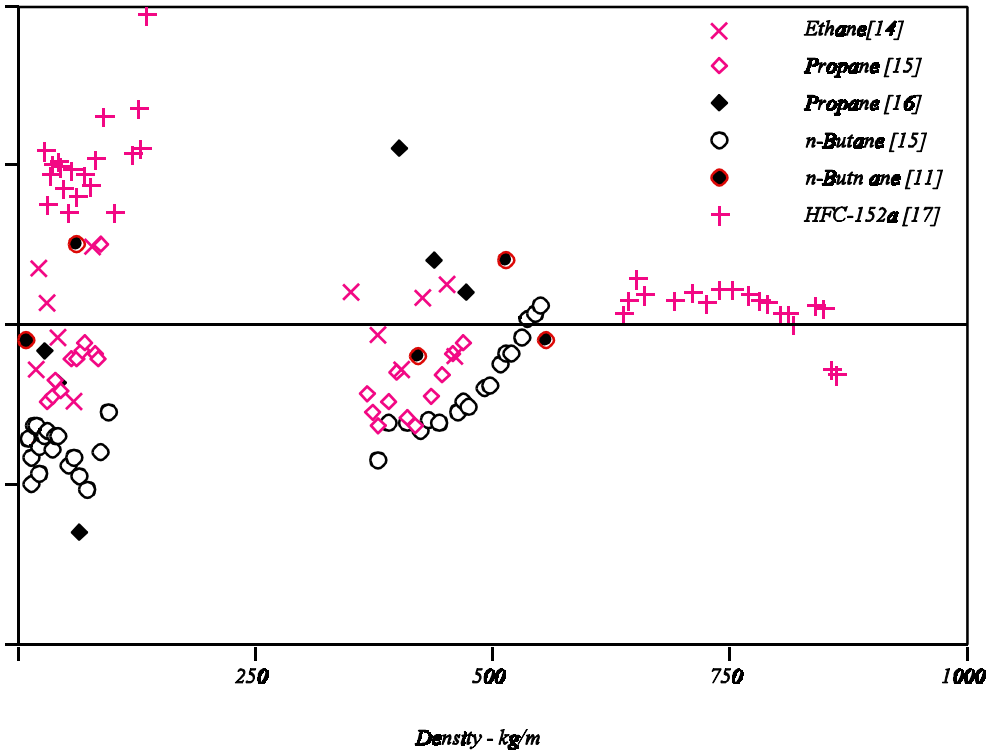
Ethane[14]
Propane [15]
Propane [16]
n-Butane [15]
n-Butn ane [11]
HFC-152a [17]
250
500
750
1000
Density - kg/m

Figure 1. Schematic Diagram of a Vibrating-Tube Densimeter.

Figure2. Comparisons of experimental density data for ethane, propane, n-butane, and HFC-152a to high accuracy correlation [18-21].